JOURNAL OF GEOPHYSICAL RESEARCH, VOL. 105, NO. D18, PAGES 22,671–22,684, SEPTEMBER 27, 2000

Model of tropospheric ion composition: A first attempt

G. Beig

Indian Institute of Tropical Meteorology, Pune, India

Guy P. Brasseur

Max Planck Institute for Meteorology, Hamburg, Germany
National Center for Atmospheric Research, Boulder, Colorado

Abstract. Recent atmospheric ion composition measurements in the troposphere have revealed the presence of several new families of ions below the tropopause, which had not been observed above this level. In a chemical model of tropospheric positive ions, several new channels are proposed to explain this observation, and the presence of very heavy clustered aerosol ions (charged ultrafine particles) are considered. Parent neutral compounds, that are responsible for the formation of positive cluster ions in the troposphere, include ammonia, pyridine, picoline, lutidine, acetone, etc. Model results show that the clustered aerosol ions are dominant near the surface, above which pyridinated cluster ions are most abundant up to about 5 km altitude. Above 7 km, ions having acetone as parent neutral species are in majority. Ammonia and methyl cyanide cluster ions are found to be less abundant as compared to the above. Above 13 km the relative abundance of methyl cyanide cluster ions is rapidly increasing, which suggests that the present model results conform with stratospheric ion models. Experimental data suggest, however, that the concentration of pyridinated compounds is highly variable from one location to another and that the relative abundance of ammonia cluster ions could be high in some remote environments. Similarly, our model shows that $NO_3^-.HNO_3$ $(H_2O)_n$, HSO_4^-, and NO_3^--core families of ions are the most abundant negative ions in the troposphere during nighttime. The first family dominates below 6 km, whereas the second type dominates between 6 and 10 km. NO_3^--core ions are the most abundant ions above 10 km. However, some observational data suggest a dramatic increase in the concentration of sulfuric acid vapor, malonic acid, and methane sulfonic acid during daytime with a related change in the negative ion composition. Our model suggests that under these conditions HSO_4^--core ions are the dominant ions below 10 km altitude.

1. Introduction

During the past 2 decades, considerable progress has been made toward achieving a better understanding of ion chemistry below the stratopause. Until recently, many ion composition measurements have been reported for the stratosphere [*Arijs*, 1992, and reference therein], while little attention was given to ion composition in the troposphere. However, tropospheric ions play an important role because they influence the electrical conductivity of the atmosphere and their recombination could be a source of ultrafine aerosol particles in the lower atmosphere [*Mohnen*, 1971; *Arnold*, 1982; *Turco et al.*, 1998; *Yu and Turco*, 2000] The first ion composition measurements near the ground reported by *Eisele* [1983] revealed the presence of unidentified positive ions with masses of 80 and 94 amu. Thereafter, a few more high-resolution mass spectrometric measurements of naturally occurring tropospheric ions were performed by *Perkins and Eisele* [1984], *Arnold et al.* [1984], *Eisele and McDaniel* [1986], *Eisele* [1986], *Eisele* [1989a, b], and *Tanner and Eisele* [1991].

Fifteen years ago, *Heitmann and Arnold* [1983] reported the first measurements of negative ions in the troposphere and suggested that the majority of ground level and lower tropospheric negative ions belong to several ion families including NO_3^- $(HNO_3)_n$ $(H_2O)_m$, as well as NO_3^- and HSO_4^- core ions. Recently, *Eisele and Tanner* [1993] observed a substantial day-night variation in sulfuric acid which should have a considerable influence on the negative ion composition. Specifically, they noticed that daytime gas-phase H_2SO_4 concentrations at ground level are at least an order of magnitude larger than nighttime values. The reduction in the abundance of gas-phase sulfuric acid after sunset results from the shut off of the photooxidation mechanisms which convert SO_2 into H_2SO_4, while the uptake of sulfuric acid vapors onto aerosols remains rapid [*Eisele and Tanner*, 1993]. Similarly, the concentration of malonic acid ($C_3H_4O_4$ or MA) and methane sulfonic acid (CH_4SO_3 or MSA) is also reported to undergo diurnal variations [*Eisele and Tanner*, 1993]. As a result, the HSO_4^- core ions are expected to be a dominant family during daytime while a minority family during nighttime

Several of the early ion composition measurements resulted in the identification of NH_4^+ $(H_2O)_m$ positive ions. Various heavy ion mass peaks were also observed, but their identification remained speculative Improved measurement techniques by *Eisele* [1988] have led to the identification of heterocyclic nitrogen-containing organic molecules, primarily pyridine (C_5H_5N), picoline (or methylpyridine $C_5H_4(CH_3)N$), and lutidine (or dimethylpyridine $C_5H_3(CH_3)_2N$), as the parent neutral species for observed positive ion masses 80, 94, and 108, respectively. Alkaline species and

Paper number 2000JD900119.
0148-0227/00/2000JD900119$09.00

other heavy ions were also detected in the positive ion spectrum. On the basis of this study it has become increasingly evident that, in most environments, the most abundant positive ions are not $NH_4^+ (H_2O)_n$ but pyridine and other alkaline-containing ions. However, in a more recent study, *Tanner and Eisele* [1991], while not ruling out the presence of pyridinated cluster ions, again found that ammonia cluster ions may be abundant and therefore cannot be ignored Moreover, the concentration of pyridinated compounds is highly variable from one location to another due to their relatively short lifetime (days to weeks) and the geographical variations in their sources. Hence, in locations where the concentration of pyridinated compounds is small (e.g,. the ocean), ammonia and other cluster ions may be dominant as observed by *Tanner and Eisele* [1991]. In addition, several heavy ion peaks are still unidentified, awaiting improved and more sensitive instrumental techniques.

Owing to the above uncertainties in the ion composition measurements, not much progress has been made so far in the development of theoretical models for tropospheric ions. The early models for tropospheric positive and negative ions developed by *Huertas and Fontan* [1975] and *Huertas et al.* [1978] were based on relatively simple and incomplete chemical schemes. More recent attempts made by *Kawamoto and Ogawa* [1986] and, more recently, by *Luts and Salm* [1994] and by *Luts* [1995] have considered an increasingly important number of tropospheric ions and ion reactions. The model study of *Beig and Brasseur* [1999] has shown that ion composition in the troposphere could be substantially modified as a result of anthropogenic perturbations.

Laboratory measurements of several important reaction rates of interest to tropospheric ion chemistry have become available during the last 2 decades [e.g., *Viggiano et al.*, 1982; 1988a; b] and allow more detailed model studies. A few years ago, *Arijs* [1992] reviewed the present status of ion composition and stressed the need for more detailed studies on troposphere ion processes. The aim of the present study is to present a model of tropospheric positive ions in light of recent measurements of ion composition and of reaction rates. Several new reaction channels are proposed, leading to the presence of heavy ions that remain to be experimentally identified. A model of tropospheric negative ion composition based on revised reaction rates is also presented along with some sensitivity tests. Note that much of the postulated ion-molecule chemistry has not yet been carefully studied in the laboratory and that the concentrations of organic ligands such as picoline and lutidine adopted here are based on very preliminary field studies. Our model study should therefore be viewed as a first attempt to calculate the vertical distribution of tropospheric ions.

2. Model Description and Ion Chemical Schemes

2.1. Positive Ion Scheme

The ion chemical scheme proposed in this work and used to calculate the tropospheric positive ion composition is shown in Figure 1a. The major source of ionization in the troposphere is provided by galactic cosmic rays and radioactivity (the later being important only 1–2 km above the surface). The associated ion-pair production rate has been taken from the study of *Rosen et al.* [1985]. Ions initially formed in this transfer are O_2^+ and N_2^+. However, N_2^+ is immediately converted to O_2^+ by charge exchange with O_2 and other ions are subsequently produced leading to the formation of water cluster ions $H^+ (H_2O)_r$ (known as proton hydrates or PH ions and representing the sum of all PH ions for r = 1,2....) [*Ferguson et al.*, 1979]. All the reaction rates associated with the formation of proton hydrates are fairly well known from laboratory studies and are used in the present model as in the study of *Beig et al.* [1993a]. Reaction paths affecting $H^+ (H_2O)_r$ in the troposphere are believed to be more complex than those occurring in the stratosphere. Possible paths are shown in Figure 1a and the rate constants for the reactions ignored in the study of *Beig et al.* [1993a] and used in the present study are given in Table 1. The reaction rate for the conversion of PH to $H^+(CH_3CN)_p (H_2O)_n$ (known as methyl cyanide cluster ions or non-proton hydrates (NPH) and representing the sum of all NPH ions with p,n =1,2.....) has been measured in the laboratory by *Viggiano et al.* [1988b]. These values are used in the present study. This particular path is important mostly above the

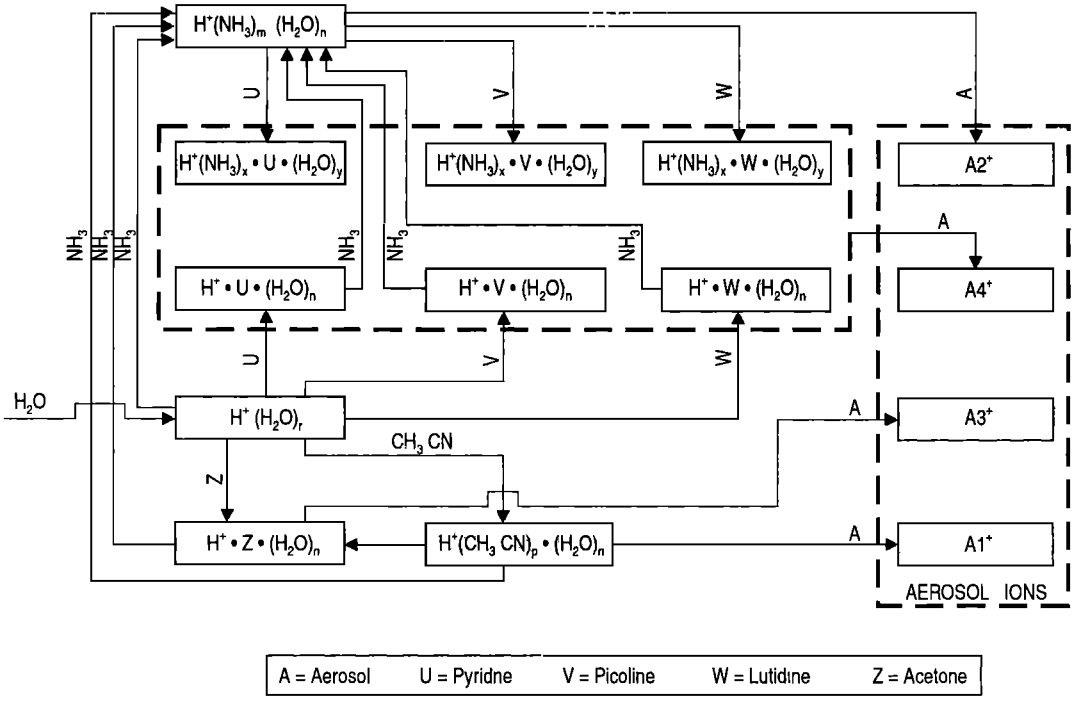

Figure 1a Tropospheric positive ion chemical scheme used in the present model.

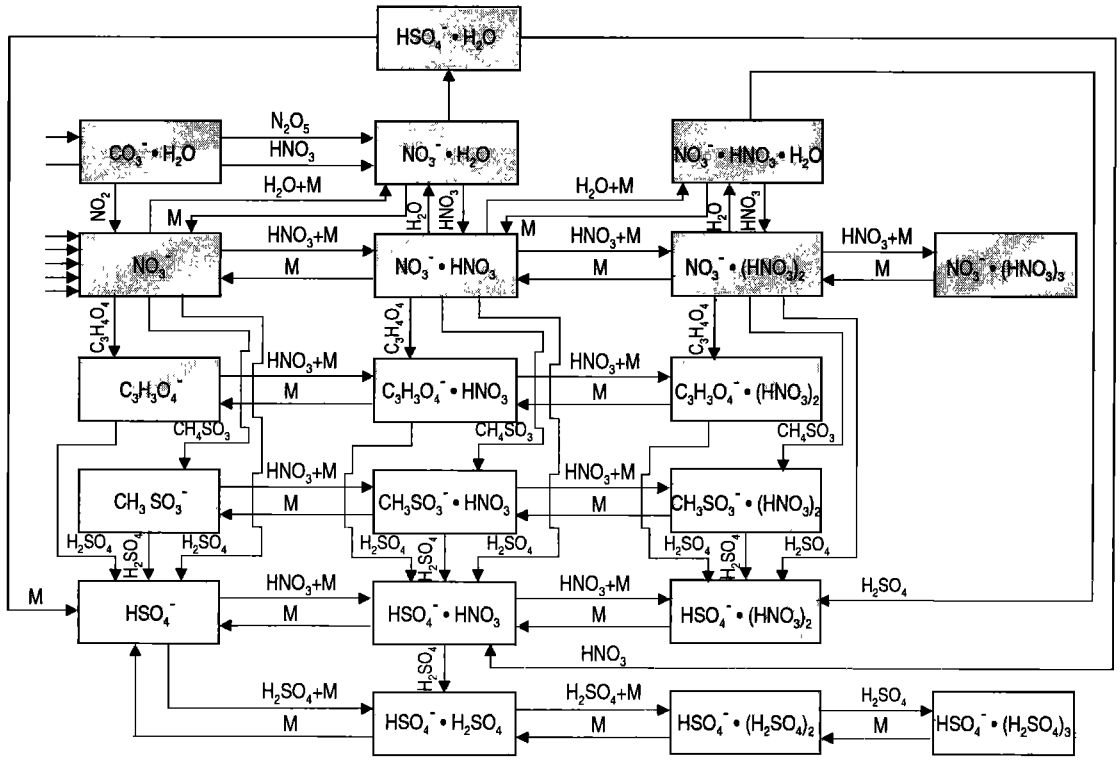

Figure 1b. Tropospheric negative ion chemical scheme used in the present model.

tropopause [*Beig et al.*, 1993a]. In the troposphere, however, the reaction of PH ions with several alkaline compounds with high proton affinity, as shown in Figure 1a, should be faster than the reaction with methyl cyanide (CH_3CN). Examples are provided by the reactions of PH with ammonia (NH_3) and acetone (CH_3COCH_3) whose rates (k_1 and k_2) are known from recent laboratory measurements [*Viggiano et al.*, 1988b]. Resultant ion families are $H^+(NH_3)_m(H_2O)_n$ and $H^+(CH_3COCH_3).(H_2O)_n$ (with m and n = 1,2,3,....., and are named here ammonia cluster ions and acetone cluster ions, respectively). The formation mechanism for other types of ions, such as $H^+(NH_3)_x.(Pyridine).(H_2O)_y$ (ion type no.1); $H^+(NH_3)_x.(Picoline).(H_2O)_y$ (ion type no.2) and $H^+(NH_3)_x.(Lutidine).(H_2O)_y$ (ion type no.3), whose presence near the surface has been suggested from ion mass spectrometry measurements [*Eisele*, 1988], is not well established. We suggest that, for example, $H^+(NH_3)_x.(Pyridine).(H_2O)_y$ ions may be formed via two different reaction paths. In the first of them, the PH ions are initially converted to ammonia cluster ions (reaction k_1 in Table 1)

$$H^+(H_2O)_n \xrightarrow{NH_3} H^+(NH_3)_m(H_2O)_n \qquad (1a)$$

and subsequently to pyridinated clusters (reaction k_8):

$$H^+(NH_3)_m(H_2O)_n \xrightarrow{Pyridine} H^+(NH_3)_x.(Pyridine)(H_2O)_y . \qquad (1b)$$

Similar reactions can be considered for ion families involving picoline (2) and lutidine (3). In these reaction schemes it is not clear as to how multiples of NH_3 and H_2O molecules arise. The reaction rates for this first path are known and make this reaction channel a fast and straightforward mechanism for the production of ion family 1 and also probably for families 2 and 3 In the second path, which is believed to be much less efficient, the initial step is a reaction with pyridine (reaction k_{11})

$$H^+(H_2O)_r \xrightarrow{Pyridine} H^+(Pyridine)(H_2O)_n \qquad (2a)$$

followed by a substitution reaction with ammonia (reaction k_{12})

$$H^+.(Pyridine)(H_2O)_n \xrightarrow{NH_3} H^+(NH_3)_m(H_2O)_n \qquad (2b)$$

and a subsequent addition of pyridine as in reaction (1b)

Reaction (2a) is considered as efficient on the basis of the measurement of rate constant (k_{11}) [*Viggiano et al.*, 1988b]. The ion family resulting from reaction (2a) is $H^+.(Pyridine).(H_2O)_n$ (type 4) Similarly, $H^+.(Picoline).(H_2O)_n$ (type 5) and $H^+.(Lutidine).(H_2O)_n$ (type 6) may be formed. Note that no information is available for the rate at which the NH_3 substitution reaction (2b) takes place. Because pyridine has a higher proton affinity than ammonia, this reaction is probably slow. A rate constant of 10^{-11} cm^3 s^{-1} has been assumed and probably represents an upper limit. Similarly rate constants k_9 and k_{10} of the paths proposed for the conversion of PH to $H^+.(Picoline).(H_2O)_n$ and $H^+.(Lutidine).(H_2O)_n$ ions are not known and are assumed to be equal to the rate of analogous path, k_{11} (without temperature dependence factor), which has been measured in the laboratory Ions (1), (2), and (3) are eventually formed from $H^+(NH_3)_m(H_2O)_n$ reaction (1b). The associated reaction rate constants k_6 and k_8 have been studied in the laboratory by *Viggiano et al.* [1988a] for various values of m and n. Rate constant k_7 (which is still unknown) is assumed to be identical to k_8. The sum of six ion families, (1), (2), (3), (4), (5), and (6) represented inside the box in Figure 1a will be referred to as "Pyridinated Cluster Ions." The sum of ions (1) and (4) will be called "Pyridine Cluster" ions, (2) and (5) "Picoline cluster" ions, and (3) and (6) "Lutidine cluster" ions. Note that no reverse reactions are considered in our ion scheme because, as indicated above, the proton affinity of alkaline compounds is higher than that of H_2O or NH_3. In the present work, we also suggest that some very heavy ions may be

Table 1. Reactions Supplementary to the Reactions Adopted by *Beig et al* [1993a, b] and Corresponding Reaction Rate Constants

Reaction	Rate Constant, $cm^3 s^{-1}$	Reference
$H^+(H_2O) + H_2O + M \rightarrow H^+(H_2O)_r$	$R_1 = 3.5 \times 10^{-27} (300/T)^2$ [M]	*Lau et al.* [1982]
$H^+(H_2O)_r + CH_3CN \rightarrow H^+(CH_3CN)_p(H_2O)_n$	$R_2 = 3.06 \times 10^{-9} (300/T)$	*Viggiano et al.* [1988b]
$H^+(H_2O)_r + NH_3 \rightarrow H^+(NH_3)_m(H_2O)_n$	$k_1 = 1.91 \times 10^{-9} (300/T)^{0.39}$	*Viggiano et al.* [1988b]
$H^+(H_2O)_r + CH_3COCH_3 \rightarrow H^+(CH_3COCH_3)(H_2O)_n$	$k_2 = 2.04 \times 10^{-9} (300/T)^{0.59}$	*Viggiano et al.* [1988b]
$H^+(CH_3COCH_3)(H_2O)_n + NH_3 \rightarrow H^+(NH_3)_m(H_2O)_n$	$k_3 = 2 \times 10^{-9}$	*Hauck and Arnold* [1984]
$H^+(CH_3CN)_p(H_2O)_n + CH_3COCH_3 \rightarrow H^+(CH_3COCH_3)(H_2O)_n$	$k_4 = 1.8 \times 10^{-9}$	*Hauck and Arnold* [1984]
$H^+(CH_3CN)_p(H_2O)_n + NH_3 \rightarrow H^+(NH_3)_m(H_2O)_n$	$k_5 = 1.8 \times 10^{-9}$	*Schlager et al.* [1983]
$H^+(NH_3)_m(H_2O)_n$ + picoline $\rightarrow H^+(NH_3)_x$(picoline)$(H_2O)_y$	$k_6 = 2.6 \times 10^{-9} (300/T)^{0.7}$	*Viggiano et al.* [1988a]
$H^+(NH_3)_m(H_2O)_n$ + lutidine $\rightarrow H^+(NH_3)_x$(lutidine)$(H_2O)_y$	$k_7 = 2 \times 10^{-9}$	assumed
$H^+(NH_3)_m(H_2O)_n$ + pyridine $\rightarrow H^+(NH_3)_x$(pyridine)$(H_2O)_y$	$k_8 = 2.1 \times 10^{-9} (300/T)^{0.7}$	*Viggiano et al* [1988a]
$H^+(H_2O)_r$ + picoline $\rightarrow H^+$(picoline)$(H_2O)_n$	$k_9 = 2 \times 10^{-9}$	assumed
$H^+(H_2O)_r$ + lutidine $\rightarrow H^+$(lutidine)$(H_2O)_n$	$k_{10} = 2 \times 10^{-9}$	assumed
$H^+(H_2O)_r$ + pyridine $\rightarrow H^+$(pyridine)$(H_2O)_n$	$k_{11} = 2.08 \times 10^{-9} (300/T)^{0.89}$	*Viggiano et al.* [1988b]
$H^+X(H_2O)_n + NH_3 \rightarrow H^+(NH_3)_m(H_2O)_n$	$k_{12} = k_{13} = k_{14} = 1 \times 10^{-11}$	assumed
$NO_3^- + C_3H_4O_4 \rightarrow C_3H_3O_4^-$	$R29 = 2.5 \times 10^{-9}$	assumed [a]
NO_3^- $(HNO_3) + C_3H_4O_4 \rightarrow C_3H_3O_4^-$ (HNO_3)	$R30 = 2 \times 10^{-9}$	assumed [a]
NO_3^- $(HNO_3)_2 + C_3H_4O_4 \rightarrow C_3H_3O_4^-$ $(HNO_3)_2$	$R31 = 1 \times 10^{-9}$	assumed [a]
$NO_3^- + CH_4SO_3 \rightarrow CH_3SO_3^-$	$R32 = 2.5 \times 10^{-9}$	assumed [a]
NO_3^- .$(HNO_3)+CH_4SO_3 \rightarrow CH_3SO_3^-$ (HNO_3)	$R33 = 2 \times 10^{-9}$	assumed [a]
NO_3^- .$(HNO_3)_2+CH_4SO_3 \rightarrow CH_3SO_3^-$ $(HNO_3)_2$	$R34 = 1 \times 10^{-9}$	assumed [a]
$C_3H_3O_4^- + HNO_3+M \rightarrow C_3H_3O_4^-$ HNO_3	$R35 = 1 \times 10^{-26}$ [M]	assumed [b]
$C_3H_3O_4^-$ $HNO_3+M \rightarrow C_3H_3O_4^-$	$R36 = 1 \times 10^{-21}$ [M]	assumed [b]
$C_3H_3O_4^-$. $HNO_3+ HNO_3+M \rightarrow C_3H_3O_4^-$ $(HNO_3)_2$	$R37 = 1 \times 10^{-26}$ [M]	assumed [b]
$C_3H_3O_4^-$.$(HNO_3)_2+M \rightarrow C_3H_3O_4^-$ (HNO_3)	$R38 = 1 \times 10^{-18}$ [M]	assumed [b]
$CH_3SO_3^-+ HNO_3+M \rightarrow CH_3SO_3^-$ (HNO_3)	$R39 = 1 \times 10^{-26}$ [M]	assumed [b]
$CH_3SO_3^-$ $HNO_3+M \rightarrow CH_3SO_3$	$R40 = 1 \times 10^{-21}$ [M]	assumed [b]
$CH_3SO_3^-$.$(HNO_3)+HNO_3+M \rightarrow CH_3SO_3^-$ $(HNO_3)_2$	$R41 = 1 \times 10^{-26}$ [M]	assumed [b]
$CH_3SO_3^-$.$(HNO_3)_2+M \rightarrow CH_3SO_3^-$ (HNO_3)	$R42 = 1 \times 10^{-18}$ [M]	assumed [b]
$C_3H_3O_4^-+H_2SO_4 \rightarrow HSO_4^-$	$R43 = 2 \times 10^{-9}$	assumed
$C_3H_3O_4^-$.$HNO_3 + H_2SO_4 \rightarrow HSO_4^-$ (HNO_3)	$R44 = 2 \times 10^{-9}$	assumed
$C_3H_3O_4^-$.$(HNO_3)_2 + H_2SO_4 \rightarrow HSO_4^-$ $(HNO_3)_2$	$R45 = 1 \times 10^{-9}$	assumed
$CH_3SO_3^-+H_2SO_4 \rightarrow HSO_4^-$	$R46 = 2 \times 10^{-9}$	assumed
$CH_3SO_3^-$ $HNO_3+H_2SO_4 \rightarrow HSO_4^-$.$HNO_3$	$R47 = 2 \times 10^{-9}$	assumed
$CH_3SO_4^-$.$(HNO_3)_2+H_2SO_4 \rightarrow HSO_4^-$ $(HNO_3)_2$	$R48 = 1 \times 10^{-9}$	assumed
NO_3^-.$HNO_3.H_2O+H_2SO_4 \rightarrow HSO_4^-$ $(HNO_3)_2$	$R49 = 2 \times 10^{-9}$	assumed
NO_3^- $H_2O+H_2SO_4 \rightarrow HSO_4^-$ H_2O	$R50 = 2 \times 10^{-9}$	assumed
HSO_4^- $H_2O+M \rightarrow HSO_4^-$	$R51 = 3 \times 10^{-9}$	assumed
HSO_4^- $H_2O+HNO_3 \rightarrow HSO_4^-$ HNO_3	$R52 = 3.6 \times 10^{-14}$ [M]	assumed

[a] Values of rate constants for reactions of NO_3^- core ions with MA and MSA are assumed to be the same as the rate constants of NO_3^- core ions with H_2SO_4 (as determined by *Viggiano et al* [1982]

[b] Rate constants for the forward three-body recombination reactions (reactions (R35), (R37), (R39), and (R41)) for $CH_3SO_3^-$ and $C_3H_3O_4^-$ reactions (10^{-26} $cm^6 s^{-1}$) are assumed to be the same as the corresponding recombination reactions of NO_3^- ions Rate constants for the reverse reactions (reactions (R36), (R38), (R40), and (R42)) are derived from thermodynamic considerations.

formed through the attachment of the major resultant ions (shown in Figure 1a) on tropospheric aerosols. These heavy positive aerosol clustered ions are denoted as $A1^+$, $A2^+$, $A3^+$, $A4^+$ in this figure. The composition of $A1^+$ is of the type H^+ (Aerosol) $(CH_3CN)_p$ $(H_2O)_n$ with methyl cyanide as a parent neutral compound. Similarly, attachment of aerosol with ammonia, acetone and pyridinated clustered ions constitute $A2^+$, $A3^+$, $A4^+$ ions, respectively. The concentration of these ions is likely to decrease with increasing height as the aerosol concentration decreases with altitude. It should be noted, however, that the mass of these aerosol cluster ions (ultrafine charged particles) is of the order of 10^3 to 10^4 amu, so that their mobility is very small. Hence these very heavy charged particles do not fall under the normal description of ions. It should be mentioned that, in addition to the positive ions shown in Figure 1a, several other compounds have been identified [*Tanner and Eisele*, 1991] including methyl substituted glucose amines and primary amines, etc., that form their cluster ions by proton exchange. The corresponding reaction rates and the atmospheric abundance of these ions are not yet known. Nevertheless, sensitivity tests based on rough estimates for reaction rates suggest that abundance of these ions is relatively small compared to other cluster ions. Hence, to avoid any unnecessary complication, these ions are not shown in Figure 1a. The attachment coefficient (β) for ions on aerosols depends on the radius of the condensation nuclei. The values reported in the literature range, however, from 10^{-5} to 10^{-6} $cm^3 s^{-1}$ for lighter to heavier aerosol particles. In the present work, we have adopted an effective attachment coefficient value of 5×10^{-6} $cm^3 s^{-1}$. Sensitivity tests show that our results are not strongly affected by the choice of this working value. The formation mechanism of clustered aerosol ions ($A1^+$, $A2^+$, ...) adopted here is similar to the mechanism proposed earlier by *Datta et al.* [1987] for the middle atmosphere. The formation of such charged aerosol particles already suggested by *Arnold et al.* [1984] to explain the unidentified heavy mass peaks observed in their ion spectra.

In the model the loss of ions is assumed to occur by attachment on aerosol particles and by ion-ion recombination. The total recombination coefficient α used in the present work [*Arijs and Brasseur*, 1986; *Beig et al.*, 1993a] is expressed as

$$\alpha = 6\times10^{-8}\left(\frac{300}{T}\right)^{0.5} + 1.25\times10^{-25}[M]\left(\frac{300}{T}\right)^{4} \left(cm^3 s^{-1}\right)$$

where [M] represents the neutral number density (cm^{-3}) and T is the temperature (K). In the troposphere, however, the three-body recombination is expected to dominate.

2.2. Negative Ion Scheme

The chemical scheme for tropospheric negative ions proposed and used in this work is shown in Figure 1b. The first negative ion is produced by the attachment of a free electron to an oxygen molecule resulting in the formation of the primary ion O_2^-. Subsequently, other negative ions are formed, until the so-called terminal ion NO_3^- is reached. Up to this channel the scheme adopted in the present study is the same as the scheme used by *Beig et al.* [1993b] in their model of stratospheric ions. Hence the details of the corresponding reactions are not included in Figure 1b. From NO_3^- onward, our proposed scheme includes several new channels, which are important specifically for tropospheric altitudes. Five major families of ions can be identified: (1) NO_3^--core ions having HNO_3 as ligands; (2) HSO_4^--core ions having HNO_3 and H_2SO_4 as ligands; (3) $NO_3^-.HNO_3.H_2O$ type of ions; (4) $C_3H_3O_4^-$-core ions having HNO_3 as ligands; and (5) $CH_3SO_3^-$-core ions having HNO_3 as ligands; $NO_3^-(H_2O)_n$ and CO_3^--core ions have also to be considered. Note that the $NO_3^-.HNO_3.H_2O$ ion is treated separately from the other NO_3^--core ions (i.e., $NO_3^-(HNO_3)_n$) to highlight its dominant role in the troposphere. The other NO_3^--core ions are dominant in the stratosphere where the abundance of water vapor is low.

When NO_3^- combines with HNO_3, then $NO_3^-.HNO_3$ is formed which undergoes further clustering with HNO_3 to form $NO_3^-.(HNO_3)_n$ (n=2,3). Sulfate is introduced into the negative ion chemistry by reaction of nitrate core ions with H_2SO_4 to form $HSO_4^-.(HNO_3)_n$ (n=0,1,2) ions and clustering of HSO_4^- with H_2SO_4 to form $HSO_4^-.(H_2SO_4)_n$ (n = 0, 1, 2) ions. The $NO_3^-.HNO_3.H_2O$ ion is formed by the reaction of $NO_3^-(HNO_3)_n$ with H_2O. The reaction rates associated with the formation of these ions are the same as in the study of *Beig et al.* [1993b]. $NO_3^-.H_2O$ and $NO_3^-.HNO_3.H_2O$-type ions are also assumed to react with sulfuric acid to form HSO_4^- core ions. *Eisele* [1989b] and *Tanner and Eisele* [1991] have reported that methane sulfonic acid (MSA), CH_4SO_3, and malonic acid (MA), $C_3H_4O_4$, which are more acidic than nitric acid, are also capable of replacing NO_3^- provided that their abundance is sufficiently high. In the present scheme (Figure 1b), it is proposed that the reaction of NO_3^--core ions with malonic acid and methane sulfonic acid leads to $C_3H_3O_4^-$ and $CH_3SO_3^-$-core ions (with subsequently HNO_3 as ligands), respectively. However, both ion families rapidly react with H_2SO_4 (which is more acidic) to form HSO_4^- core ions as shown in Figure 1b. The rate at which NO_3^- reacts with CH_4SO_3 is not known but is believed to be close to the collision rate, as for several other proton exchange reactions. Hence, in the present case, analogous reaction rates are adopted for all these unknown channels. Finally, as in the case of positive ions, it is assumed (not shown in Figure 1b) that the major negative ions can attach on ultrafine aerosol particles present in the troposphere. As little information is available on the attachment coefficients, we use for these coefficients a working value of 5×10^{-6} cm^3 s^{-1} as in the case of positive ions.

The reaction rates for most of the channels included in the present model are taken from the earlier model study of *Beig et al.* [1993b] and the reader is referred to this paper for further details. Table 1, however, provides the values of the rate constants for the additional reactions adopted here, and specifically for those not included in the study of *Beig et al* [1993b]. As most of these rate constants have not yet been measured, several assumptions have been made For example, the rate constants of reactions between NO_3^- and its cluster ions with methane sulfonic acid and malonic acid (reactions (R29)–(R34)), which are probably close to the collision rate constants, are assumed to be the same as for similar reactions with sulfuric acid Reactions (R49)–(R52) are assumed to be proceeding with the same rate constant as the analogous reactions of NO_3^- core ions with H_2SO_4. In the case of reactions (R35)-(R42), rate constants of 10^{-26} cm^6 s^{-1} are adopted for the forward three-body reactions, while for the reverse reactions the rate constants is derived from thermodynamic considerations. Owing to the lack of experimental data, no high-pressure limit is assumed for the forward rate constants; the calculated ion concentrations depend, however, primarily on the equilibrium constants between the forward and reverse reactions rather than the absolute value of the rate constants. Finally, it is assumed that other species whose mass peaks have been identified by *Eisele and Tanner* [1990] (including $SO_4NO_2^-$, $SO_4NO_3^-$, sarcosine, etc.) have little impact on negative ion chemistry. Hence these ions are neglected in the present scheme to avoid further complications. The production rate of negative ions by cosmic rays and radioactive decay as well as the loss rate due to recombination and attachment on aerosols, are considered to be the same as in the case of positive ions (see section 2.1).

In the scheme proposed here, a total of 20 positive ions (Figure 1a shows only the 14 most important ions) and 29 negative ions (Figure 1b shows only 19 ions) is considered. The continuity equations of all the ions are solved for steady state conditions, using a matrix inversion method for both positive and negative ions, respectively [see e.g., *Beig et al.*, 1993a, b]. Calculations are performed from the surface to the altitude of 15 km (with a 1 km vertical resolution) for a particular season and for midlatitude conditions since most existing observational data are provided by measurements made at 44°N.

3. Neutral Species

Several minor neutral constituents play an important role in determining the ion composition of the troposphere. These include water vapor, methyl cyanide, ammonia, acetone, pyridine, picoline and lutidine (in the case of positive ions), and nitric acid, sulfuric acid, water vapor, methane sulfonic acid, and malonic acid (in the case of negative ions). There are many other species, which take part in tropospheric ion chemistry, but their role does not seem to be dominant. Most of the vertical profiles of the neutral species influencing the ion model are derived from a two-dimensional model [*Brasseur et al.*, 1990] which treats radiation, dynamics, and chemistry interactively.

The vertical profiles of the mixing ratio for major neutral species, important for positive ion composition, are shown in Figure 2a. This figure shows that the mixing ratio of methyl cyanide (CH_3CN) decreases slowly with increasing height. The calculated concentrations are roughly in agreement with the experimental data presented by *Ingels et al.* [1987] and *Snider and Dawson* [1984]. Recently, however, *Schneider et al.* [1997] reported methyl cyanide mixing ratios in the troposphere that are substantially higher than in previous estimates. If correct, these high concentrations imply a stronger surface source or a weaker atmospheric sink of methyl cyanide than previously assumed It is currently believed that the major sources of CH_3CN are biomass burning (including tobacco smoke) and automobile exhausts [*Hamm and Warneck*, 1990]. Atmospheric destruction is due mainly to the reaction with the hydroxyl (OH) radical. The vertical profiles for all the pyridinated compounds as derived from the two-dimensional model at mid-latitude are also shown in Figure 2a. Not much is known about the atmospheric sources and sinks of pyridine, picoline and lutidine. Their concentration and hence their role for the chemistry of positive ions are probably increasing as a result of human activities [*Beig and Brasseur*, 1999] It is believed that the sources of these organic compounds are mainly the combustion of vegetation on the continents, automobile exhaust, industrial and agricultural activities, coal tars, tobacco smoke [*Graedel*, 1978], and perhaps exchanges with the ocean. These compounds are destroyed in the atmosphere mainly by the OH radical and perhaps also by O_3, HNO_3, and NO_3 [*Eisele*, 1986; 1988]. However, additional information on the sources, removal processes, and reaction rates for these species is required to better quantify the global and regional budgets of

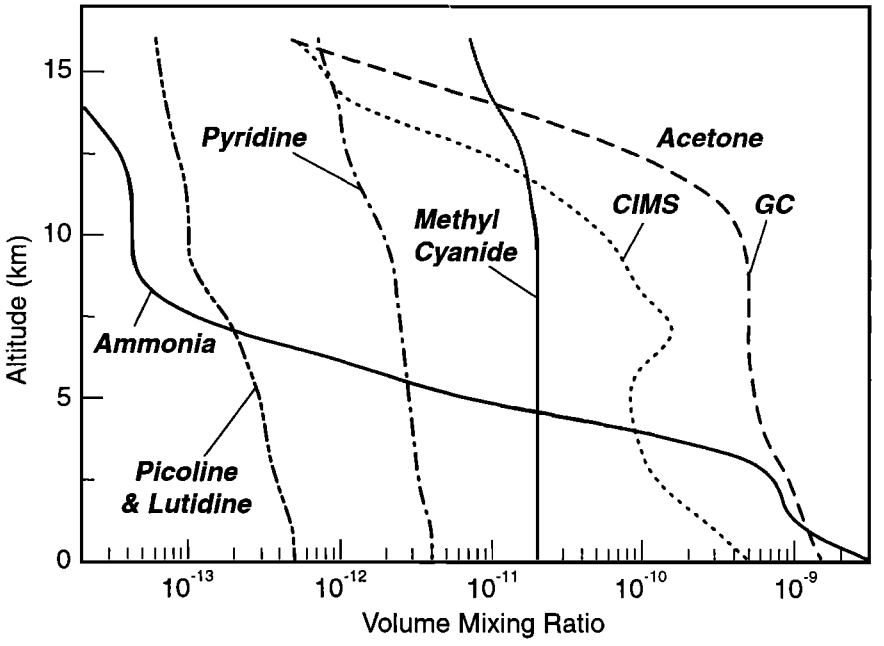

Figure 2a. Vertical distribution in the troposphere of the volume mixing ratios of ammonia, acetone, pyridine, picoline and lutidine as derived from two-dimensional model calculations or from observations (see text).

pyridinated compounds. Since the atmospheric concentration of these alkaline compounds is not well established, we have applied for all pyridinated compounds a surface boundary condition that is based on the recent estimates by *Tanner and Eisele* [1991] and *Eisele* [1988]. A value of 4 parts per trillion by volume (pptv) is adopted for pyridine, and 0.4 ppt for picoline and lutidine. The rate constant for the reaction of pyridine with OH is taken as 5 x 10^{-13} cm^3 s^{-1} and that of picoline and lutidine with OH is assumed to be 5 x 10^{-12} cm^3 s^{-1}. Reaction rates of these compounds with ozone and HNO_3 are taken as 1 x 10^{-20} cm^3 s^{-1} and 5 x 10^{-16} cm^3 s^{-1}, respectively. These compounds may also react with some NO_x species, but these reactions are not likely to have any significant role, and hence are not considered in the present model. The fact that the concentration of pyridine is 1 order of magnitude greater than that of picoline and lutidine is mainly due to the fact that the loss rate of pyridine with OH is 1 order of magnitude lower than that of picoline and lutidine. As shown by Figure 2a, the volume-mixing ratio of pyridine (4 pptv at the surface) falls off slowly with height. Similar variations with height are found for picoline and lutidine.

The vertical distribution of the species which are not included in the two-dimensional model are taken from recent experimentally derived data. For example, the vertical profile of ammonia is based on the indirect determination by *Ziereis and*

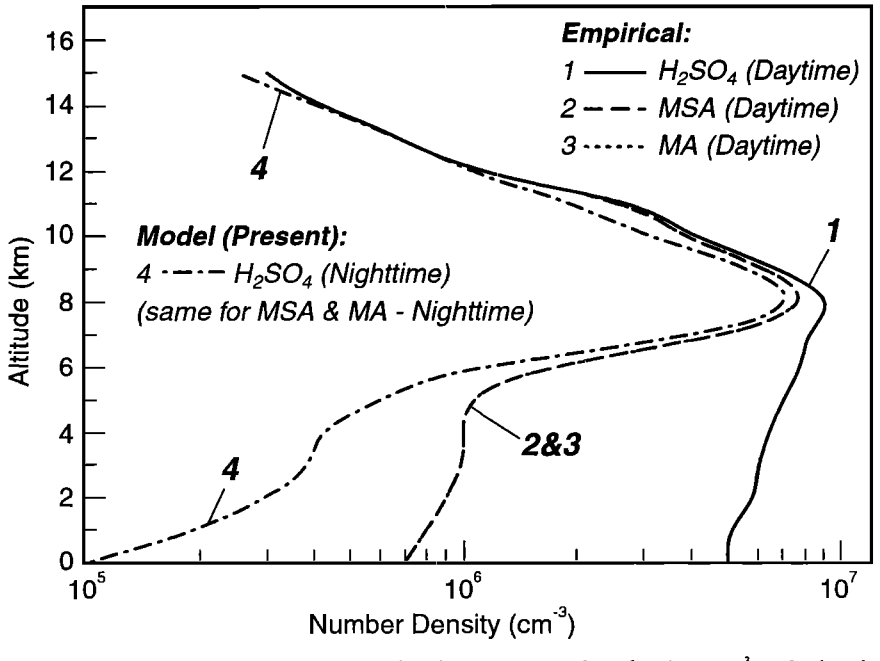

Figure 2b. Vertical distribution of H_2SO_4, MA, and MSA vapor number density (cm^{-3}) calculated for nighttime conditions and derived empirically for daytime conditions (see text).

Arnold [1986]. In the case of acetone, two different profiles are considered. The first of them is based on the gas chromatography (GC) measurements of *Singh et al.* [1994] during the Arctic Boundary Layer Expedition (ABLE 3B). Mixing ratios observed at midlatitude during this field campaign are typically 800–1500 pptv in the boundary layer and 500 pptv in the free troposphere. These values are consistent with the mixing ratios provided by a global chemical transport model such as the Model for Ozone and Related Tracers MOZART [*Hauglustaine et al.*, 1998]. A second profile with lower mixing ratios (200–500 pptv in the boundary layer and 100–200 pptv in the free troposphere) is intended to reproduce the earlier indirect estimates of the acetone mixing ratios by *Hauck and Arnold* [1984], *Arnold et al.* [1986] and *Knop and Arnold* [1987] using a chemical ionization mass spectrometry (CIMS) technique. Except when specified otherwise, the data provided by the GC measurements will be used in the present study.

The adapted vertical distribution of the aerosol concentration is assumed to represent background (nonvolcanic) conditions and is based on the measurements of condensation nuclei by *Rosen et al* [1985]. This profile should be regarded as a crude estimate of the average aerosol distribution involved in ion chemistry. Note, however, that the aerosol load of the atmosphere is highly variable with space and time and that this variability should be reflected in the ion composition, especially in the lower troposphere where the aerosol concentration is largest

Figure 2b shows the vertical distribution of sulfuric acid vapor (H_2SO_4), methane sulfonic acid (CH_4SO_3 or MSA), and malonic acid ($C_3H_4O_4$ or MA) number densities (cm^{-3}) as obtained for nighttime conditions. *Tanner and Eisele* [1991] reported that the concentration of H_2SO_4 and MSA undergo a diurnal variation They derived from their measurements at Cheeka Peak Research Station (northwest corner of the United States) that the concentration of H_2SO_4 vapor is more than an order of magnitude smaller during nighttime than during daytime. *Jefferson et al* [1998] also observed diurnal cycles in the gas-phase concentrations of MSA and H_2SO_4 at Palmer Station, Antarctica At Mauna Loa, Hawaii, where the concentration of aerosol is much lower, the diurnal variation measured by *Tanner and Eisele* (1991) seems to be less pronounced than at the continental site of Cheeka Peak. The diurnal effect reported at continental sites is presumably be due to the suppression of the H_2SO_4 source at night (oxidation of SO_2 into H_2SO_4) and the continued presence of aerosol particle surfaces which act as a sink for gas-phase H_2SO_4. The two-dimensional model (zonally averaged) does not generate day/night variations of chemical species. Hence we have estimated the possible impact of this effect by increasing the surface concentrations of these compounds from their observed night to their day values. In this sensitivity test a surface boundary concentration of 1×10^5 cm^{-3} is adopted for sulfuric acid vapor at night, whereas a value of 5×10^6 cm^{-3} is used for daytime conditions. The resulting distributions of H_2SO_4, MSA, and MA are shown in Figure 2b: the nighttime number density of H_2SO_4 vapor increases with altitude from about 10^5 cm^{-3} at the surface to 8×10^6 cm^{-3} at 8 km, while the daytime concentration of sulfuric acid vapor exhibits a slow increase with altitude from 5×10^6 cm^{-3} at the surface to a maximum (8×10^6 cm^{-3}) at about 8 km. The daytime and nighttime concentrations of H_2SO_4 become almost identical above 8 km where the aerosol concentration becomes small. The chemical processes and reaction rates involved in the production and loss of malonic acid and methane sulfonic acid are not yet known. In addition, only a few observational estimates of concentrations of these compounds are available. *Eisele* [1989b] deduced from ion concentration ratios directly under energized power lines that malonic acid is several times more abundant than sulfuric acid. At night, this ratio is reported to drop sharply. From their measurements at Palmer Station during the austral summer, *Jefferson et al.* [1998] reported 24 hour concentrations of 9.5×10^5 cm^{-3} and 1.61×10^6 cm^{-3} (3.0×10^5 cm^{-3} and 2.7×10^5 cm^{-3}) for MSA and H_2SO_4, respectively. The concentrations of MSA observed by *Mauldin et al.* [1999] over the Pacific Ocean in the boundary layer vary typically from 1.0×10^5 cm^{-3} to 1.5×10^6 cm^{-3}.

The vertical profiles of MA and MSA in the troposphere for nighttime conditions, shown in Figure 2b, are generated using the estimates of *Tanner and Eisele* [1991] and *Eisele and Tanner* [1993]. In Figure 2b the number density of MSA at the surface is 1×10^5 cm^{-3} (night); it is assumed to vary with height in a similar manner as the sulfuric acid vapor concentration obtained from the two-dimensional model. Similarly, the concentration of MA at the surface during nighttime is assumed to be 1×10^5 cm^{-3} which is also shown in Figure 2b. For daytime the density of MA and MSA is specified as 7×10^5 cm^{-3} at the surface [*Tanner and Eisele*, 1991]; the generated vertical profiles are shown in Figure 2b. MA and MSA profiles exhibit a steady but slow increase with height up to about 5 km, above which a sharp increase is noticed followed by a concentration maximum at 8 km. The vertical profile is the same as during nighttime above 8 km altitude.

4. Results on Ion Composition and Discussion

Figure 3 shows the vertical distribution of the total ion number density (positive/negative) obtained between the Earth's surface and the altitude of 15 km. This figure shows that the ion number density increases with height from 460 cm^{-3} at the surface to about 3800 cm^{-3} at 15 km. This increase by almost an order of magnitude is due primarily to the increase with height in the ion production rate. The concentration at 15 km is in agreement with the values in the lowest level of the stratosphere derived for example by *Beig et al.* [1993a, b], suggesting that a maximum in ion density lies somewhere around 15 km. The calculated total ion number density is somewhat lower than suggested by the observations of *Rosen et al.* [1985].

4.1. Positive Ions

The vertical distribution of all the major positive ions calculated by the model is represented in Figure 4. This figure shows that the dominant ions are protonated water cluster ions of pyridine, picoline and lutidine, aerosol cluster ions and acetone cluster ions. Pyridinated cluster ions along with aerosol ions are dominant below about 6 km altitude. The aerosol cluster ions (ultrafine charged particles) are found to be the most abundant near the surface (400 cm^{-3}), but for the conditions adopted here their concentration decreases with height and reaches 270 cm^{-3} at 5 km and 26 cm^{-3} at 15 km. The concentration of pyridinated cluster ions is found to be 320 cm^{-3} near the surface and increases with height to reach a maximum (1400 cm^{-3}) at about 6 km. It decreases above this altitude, but remains nearly constant with height (~200 cm^{-3}) between 8 km and 14 km. Acetone cluster ions start to dominate above 7 km throughout the upper troposphere where concentrations are larger than 1000 cm^{-3} and reach a maximum of 3000 cm^{-3} at about 12 km. It is important to emphasize here that the concentrations of pyridinated compounds probably exhibit a strong spatial variation. With lifetimes (τ) less than a month, the local abundance of pyridine (τ = 20 days); picoline (τ = 2 days); lutidine (τ = 2 days) and hence the concentration of pyridinated cluster ions at a given location may be different from what is derived by the present model case. However, the calculated concentrations should be regarded as working values representing a general "unperturbed" case. New independent measurements (including vertical profiles) of these alkaline components are needed in order to better characterize the spatial distribution of positive ion composition. Methyl cyanide cluster ions are in the minority below 7 km. However, above this altitude, they increase rapidly with height and reach a value of 1600 cm^{-3} at 15 km. Above 14 km, CH_3CN cluster ions become the dominant ions. It is interesting to note that, with the

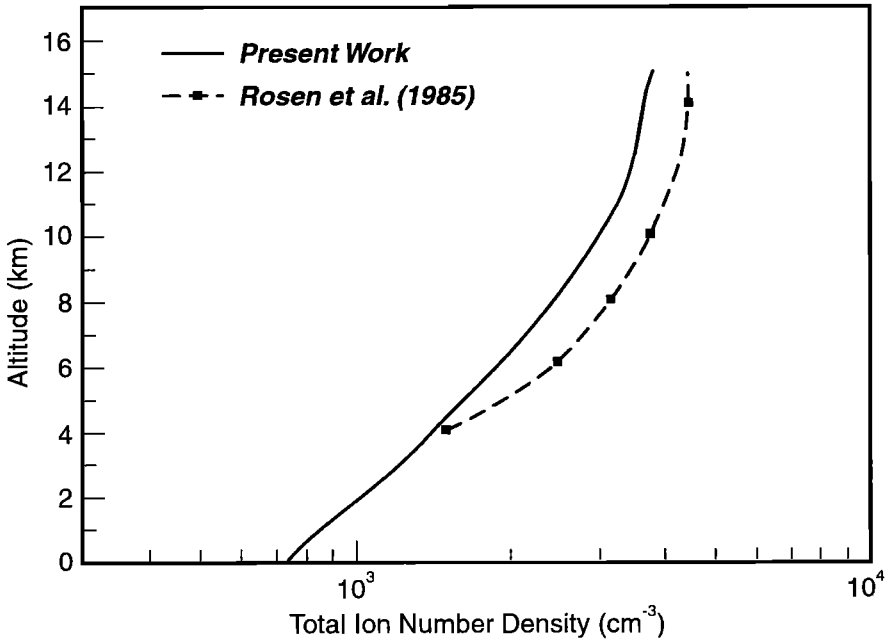

Figure 3. Comparison of the vertical distribution in the troposphere of total positive/negative ion number density (cm^{-3}) calculated at 44°N with the observational data of *Rosen et al.* [1985].

conditions adopted in the model (Figure 4), the ammonia cluster ions are never the dominant ions; their concentration increases from 10 cm^{-3} near the surface to about 100 cm^{-3} at 6 km. Above 8 km it is roughly of the order of 40 cm^{-3}. The concentration of proton hydrates is always low. It is negligible near the surface and increases with height to reach a value of 180 cm^{-3} at about 15 km.

The breakup of all six pyridinated cluster ions, as calculated by the model, is represented in Figure 5. This figure shows that the dominant ions in the pyridinated cluster ion family are $H^+(NH_3)_x$.(pyridine).$(H_2O)_y$ (type 1) below 12 km and H^+.(pyridine).$(H_2O)_n$ (type 4) above this height. The second set of dominant ions belongs to the families of $H^+(NH_3)_x$.(picoline).$(H_2O)_y$ (type 2) and $H^+(NH_3)_x$.(lutidine).$(H_2O)_y$ (type 3). The concentration of these ion families (types 2 and 3) is of the order of 40 cm^{-3} and 30 cm^{-3} near the surface, respectively. Their maximum number density is found to be around 6 km (~100 cm^{-3}). The variation with height of the concentration for these two ion families is almost identical. Above 6 km the density of these families (numbers 2 and 3) starts to decrease. It is interesting to note that the concentrations of H^+.(picoline).$(H_2O)_n$ and H^+.(lutidine).$(H_2O)_n$ families are almost negligible as compared to that of other pyridinated ions The sum of the concentration of all these ions is also shown in Figure 5.

The vertical distribution of the percentage abundance of all

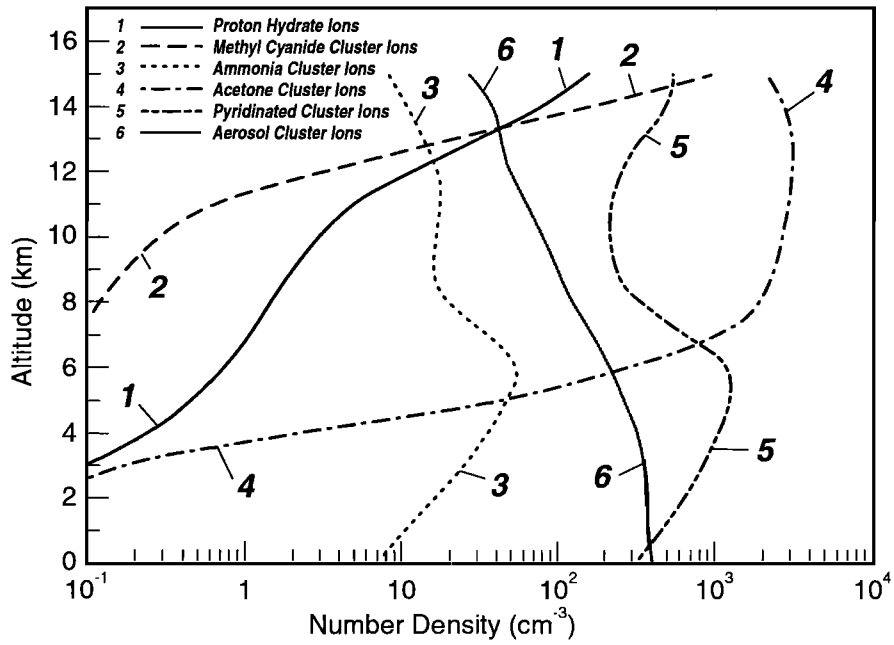

Figure 4. Vertical distribution of the major positive ion density (cm^{-3}) calculated in the model.

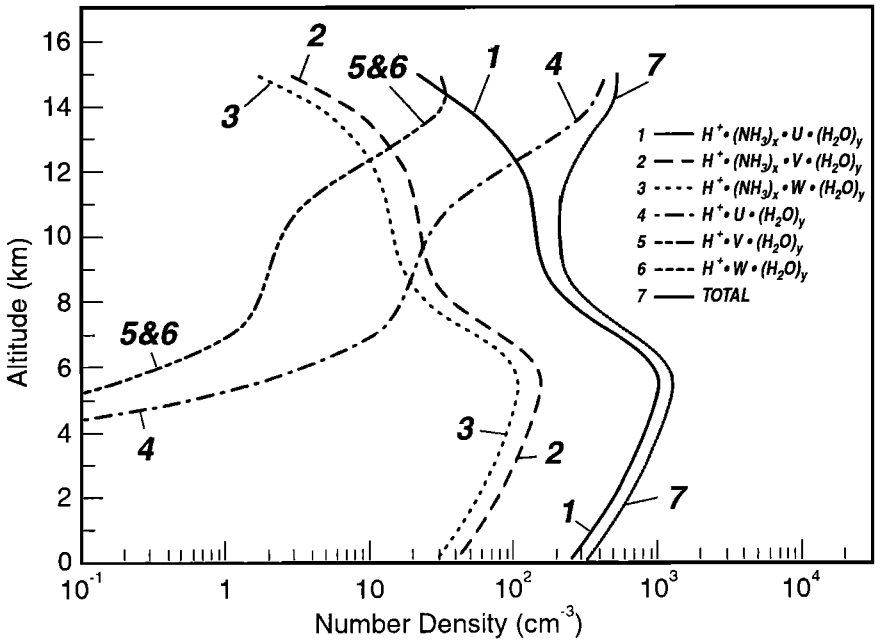

Figure 5. Vertical distribution of six pyridinated cluster ions considered in the present work and the sum of their concentration (cm^{-3}) For details, see text

major positive ions in the troposphere calculated by the model is shown in Figure 6a. In this case, the concentrations of acetone obtained by gas chromatography techniques [*Singh et al.*, 1994] have been adopted. From this figure the following conclusions can be drawn· With the conditions adopted in our model, (1) aerosol cluster ions are found to contribute more than 50% to the total ion density near the ground; (2) pyridinated cluster ions are the dominant ion family from 1 km to about 6 km and contribute 50 to 75% of the overall ion density in this atmospheric layer. The peak (75%) for this family is located at about 5 km altitude. This family contributes to about 10% in the height region of 9 km to 15 km. (3) Acetone cluster ions are found to dominate between 7 to 15 km. Their relative concentration reaches a peak value of approximately 85% at about 12 km (4) At 15 km the contribution of methyl cyanide cluster ions and acetone cluster ions are almost the same (around 40%). (5) Proton hydrate ions are always in the minority in the troposphere and their percentage abundance reaches a maximum of only 5% near the tropopause. (6) The simple ammonia cluster ions remain in the minority (maximum of 5% at 6 km). (7) All other positive ions (not shown in this figure) have negligible contributions to the total ion density. When the lower acetone concentration values deduced from ion mass spectrometry measurements [*Knop and Arnold,* 1987] are adopted (see Figure 2a), the relative abundance of the positive ions is not substantially modified.

Since large geographical differences in the concentration of pyridinated cluster ions are expected, sensitivity tests have been performed to assess the resulting changes in the percentage abundance of tropospheric ions. In Figure 6b, which is intended to be representative of a weakly polluted site (where the standard concentration of the three pyridinated compounds has been reduced by a factor 10), the dominant ion family between 1 and 6 km remains the pyridinated cluster ions with a peak in the relative abundance reduced to 55% (located at 5 km altitude). In this case, the abundance of ammonia cluster ions reaches a maximum of 20% between 5 and 6 km altitude. If we now assume that, in very remote environments, the concentration of pyridinated species is insignificant and adopt an extreme condition (zero concentration of pyridine, picoline, and lutidine in the model) (Figure 6c), the dominant ions below 6 km become ammonia cluster ions, with a maximum relative abundance of 75% near 5 km altitude In all three cases, aerosol cluster ions and acetone cluster ions remain dominant near the surface and above 7 km, respectively

4.2. Negative Ions

The concentration of the different negative ions, shown in Figure 1b, has also been calculated by the model. Figure 7 represents the vertical distribution of the percentage abundance of major negative ions obtained for nighttime conditions. It shows that, in this case, the dominant families of negative ions are NO_3^- core ions, HSO_4^- core ions, and the $NO_3^-.HNO_3.H_2O$ ion. In addition, negative aerosol cluster ions are abundant (of the order of 50% of the total ion concentration) near the surface. It is interesting to note that most of the ions below 7 km are of the type $NO_3^-.HNO_3.H_2O$. The percentage abundance of this ion is of the order of 70% between 3 and 6 km altitude. Above 6 km the concentration of $NO_3^-.HNO_3.H_2O$ decreases with height. Between 7 and 10 km, HSO_4^- core ions become dominant and contribute to 60% of the negative ions at 8.5 km altitude. The percentage abundance of NO_3^- core ions increases rapidly above 8 km. This ion becomes dominant above 10 km altitude. The other ions shown in Figure 1b contribute insignificantly to the total negative ion density

The vertical profiles of the number density of the five most abundant negative ion families calculated for nighttime conditions are shown in Figure 8. The concentration of $NO_3^-.HNO_3.H_2O$ ion (profile 3) is predicted to be 250 cm^{-3} near the surface and to reach a maximum (1400 cm^{-3}) at approximately 6 km altitude. Above 10 km the number density of this ion decreases rapidly with height. The concentration of the $NO_3^-(HNO_3)_n$ ion type, which represents the sum of all NO_3^- core ions having HNO_3 as ligands (profile 1), is very small at low altitude (less than 10 cm^{-3}) but increases with height to reach approximately 3000 cm^{-3} at 15 km. The vertical distribution of the sum of all the HSO_4^- core ions (having HNO_3 and H_2SO_4 as ligands) is also shown in this figure (profile 2). It is found that the maximum contribution to total HSO_4^- core ions is

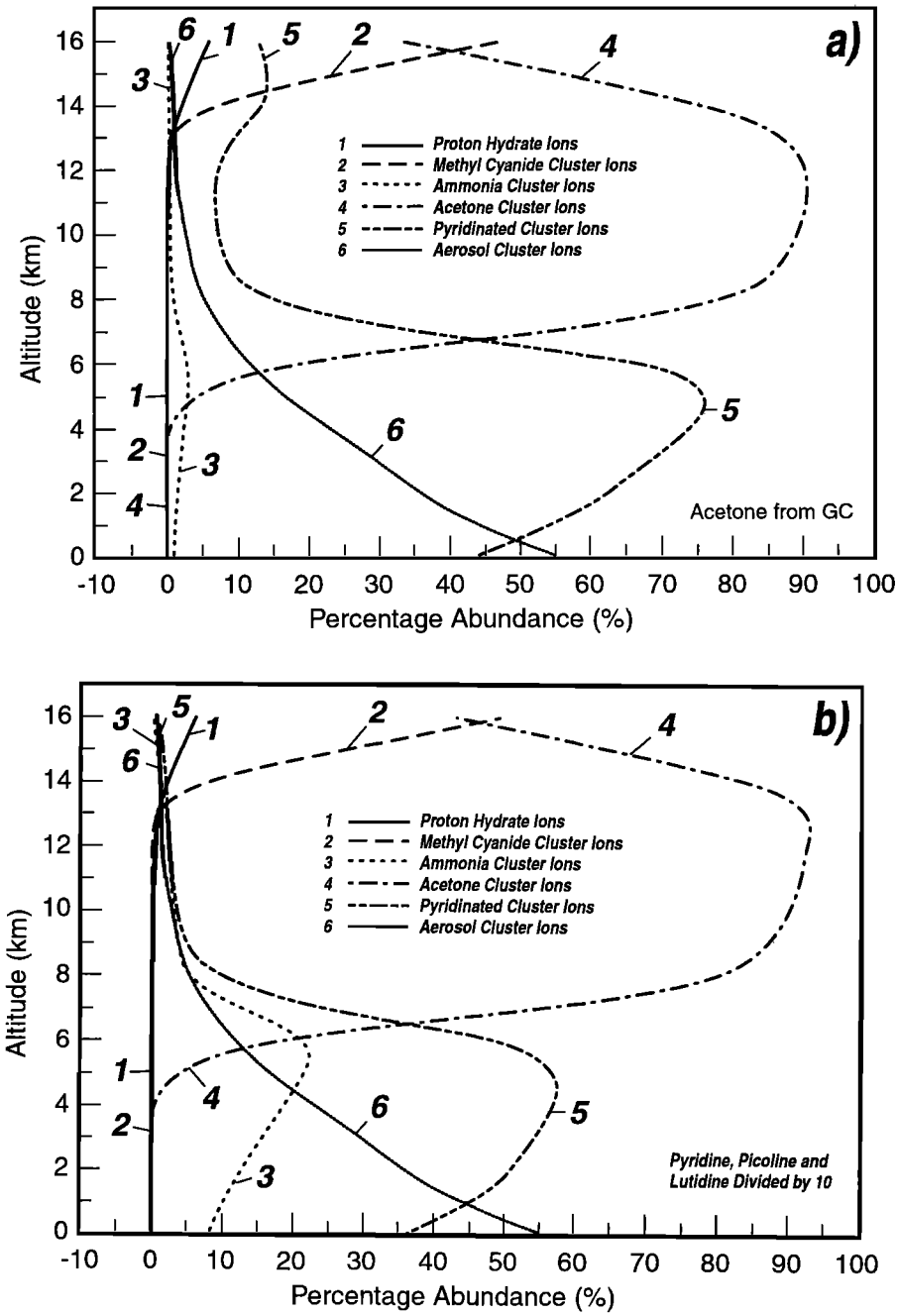

Figure 6. Vertical distributions of the percentage abundance of dominant positive ions calculated in the model: (a) acetone observations from *Singh et al.* [1994], (b) concentration of pyridinated compounds reduced by a factor of 10, and (c) concentration of pyridinated compounds set to zero.

provided by the $HSO_4^-(HNO_3)_n$ ion family, while the concentration of the $HSO_4^-(H_2SO_4)_n$ ion family is much smaller. It is noticed from Figure 8 that the concentration of HSO_4^- core ions increases with height and reaches a maximum of approximately 1400 cm^{-3} around 8 km above which it decreases slowly with height. The concentration of $C_3H_3O_4^-$ ions (MA^-) and $CH_3SO_3^-$ ions (MSA^-) (shown by profile 4 in Figure 8) are identical. They increase from 0.1 cm^{-3} at the surface to 250 cm^{-3} at 11 km. If the vertical distribution of the aerosol density suggested by *Rosen and Hofmann* (1988) is used, the calculated concentration of negative charged particles (profile 5) is typically 200 cm^{-3} between the surface and 5 km and decreases above this level.

As mentioned earlier, the concentrations of H_2SO_4, MA, and MSA seem to undergo substantial day-night variations. A sensitivity run has been made to derive the concentration of negative ion composition using reported daytime values of H_2SO_4, MA, and MSA concentrations (see Figure 2b). Figure 9 shows the relative abundance of the different negative ion types below 15 km altitude for these conditions. HSO_4^- core ions are now the most abundant ions below 10 km with a percentage abundance of typically 40–50% near the surface and 60–70% between 4 and 8 km. Below 10 km, $NO_3^-.HNO_3.H_2O$ ions contribute to approximately 20% of the negative ions. Above 10 km the most abundant ions are provided by NO_3^- core ions. With the adopted aerosol load (nonvolcanic conditions) the calculated percentage abundance of negative cluster ions is typically 40% at the surface and less than 10% above 5 km altitude. The percentage abundances of MA- and MSA-cluster ions are insignificant up to

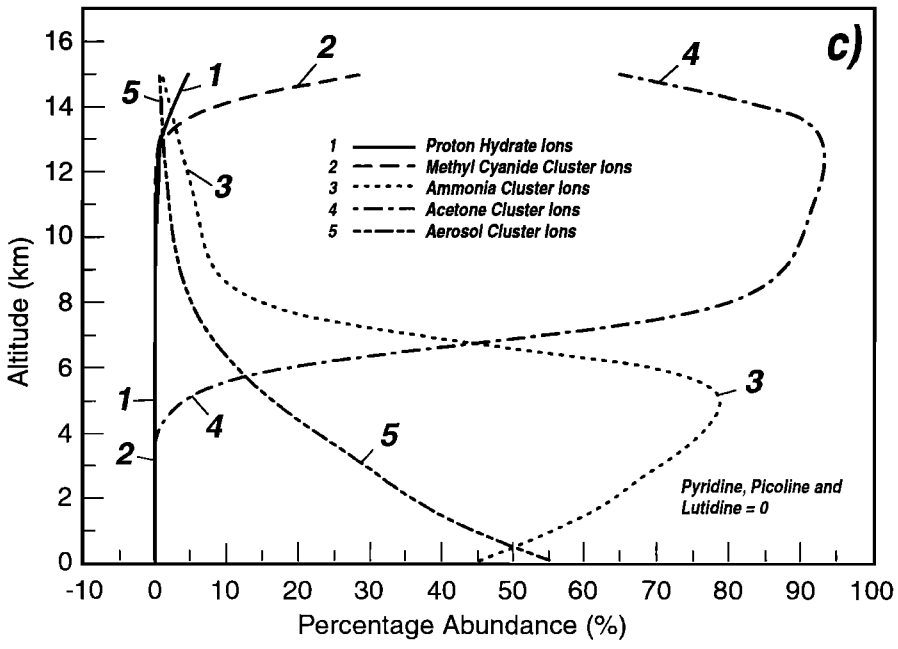

Figure 6. (continued)

6 km, but reaches approximately 10% at 11 km. Note that when the presence of aerosol particles is ignored (or for very clean air), the relative abundance of HSO_4^- core ions at the surface reaches 80% of the total ion concentration (not shown).

The vertical distributions of the ion number densities are shown in Figure 10. The number density of HSO_4^--core ions calculated for daytime conditions (profile 2) is 300 cm^{-3} near the surface, but increases with height to reach approximately 1500 cm^{-3} at 8 km. It decreases with height above this altitude. The concentration of the NO_3^--core ion family (profile 1) increases from typically 1 cm^{-3} at 2 km to 2500 cm^{-3} at 15 km altitude. In the case of $NO_3^-.HNO_3.H_2O$, the calculated density increases from 100 cm^{-3} at the surface to 500 cm^{-3} between 6 and 10 km, and decreases above 10 km. In the absence of aerosols (very clean air), the daytime concentration of HSO_4^-core ions reaches 500 cm^{-3} at the surface (not shown) *Tanner and Eisele* [1991] report daytime ion concentrations of typically 50 cm^{-3} for NO_3^- and 200–250 cm^{-3} for HSO_4^- at the Cheeka Peak Research Station in late spring. This station samples mostly very clean air from the Pacific Ocean

It is interesting to note that the calculated concentration of negative ions is strongly dependent on the rate at which $NO_3^-(H2O)_n$ and $NO_3^-.HNO_3.H_2O$ ions react with sulfuric acid reactions (R50) and (R49) The corresponding rate constants have not been measured and a value of 2 x 10^{-9} cm^3 s^{-1} is adopted for the two reactions. A calculation in which these rate constants are set to

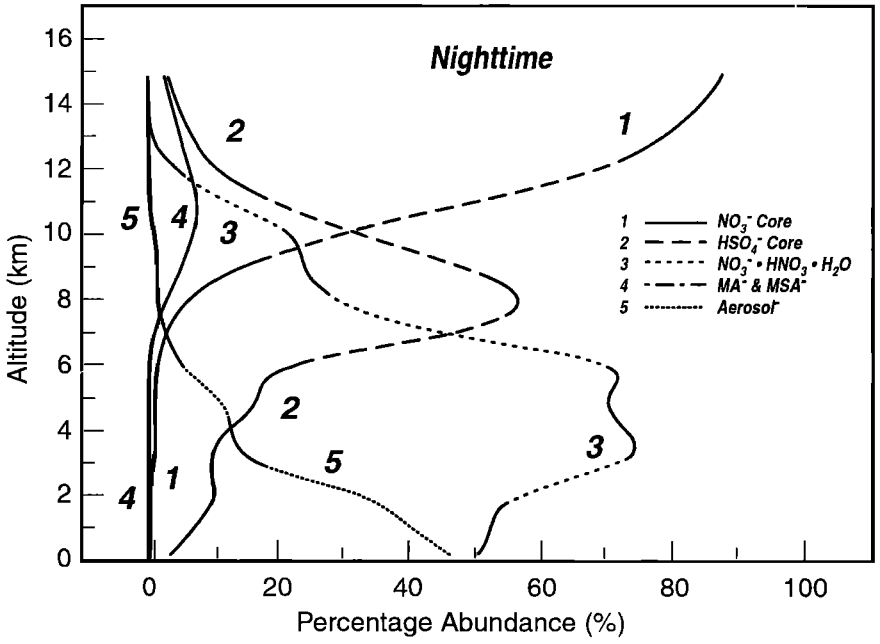

Figure 7. Height profiles of the percentage abundance of major negative ions (NO_3^--core, HSO_4^--core and $NO_3^-.HNO_3.H_2O$, MA and MSA^- clusters) as calculated for nighttime conditions.

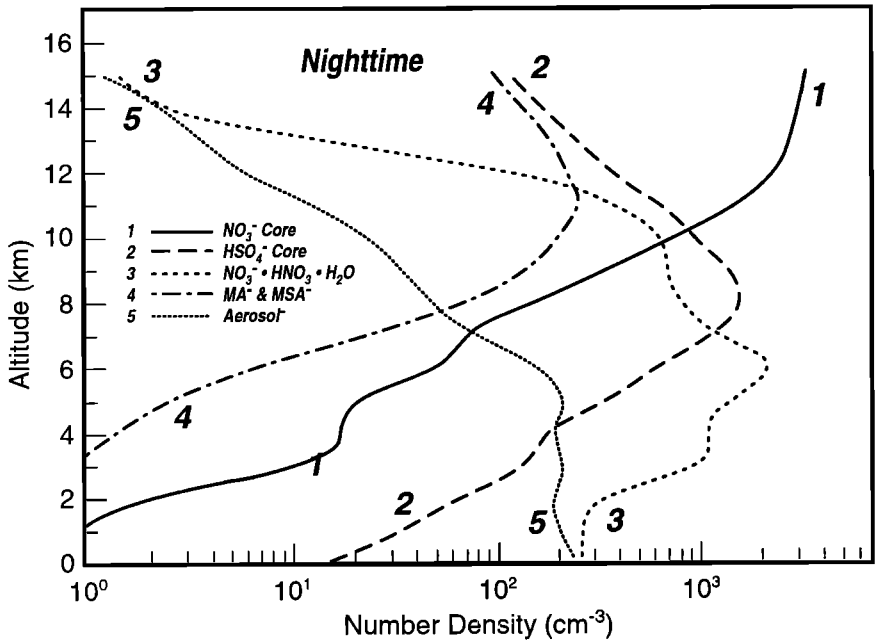

Figure 8. Vertical distribution of the concentration (cm^{-3}) of the major negative ions calculated for nighttime conditions.

zero show that, in this case, $NO_3^-.HNO_3.H_2O$ ions are dominant during daytime below 10 km altitude with a concentration at the surface 50 times higher than that of HSO_4^- core ions. Thus the calculated ion concentration values depend strongly on the rates at which $NO_3^-(H_2O)_n$ and $NO_3^-.HNO_3.H_2O$ react with sulfuric acid.

5. Concluding Remarks

The present study is a first attempt to model simultaneously positive and negative ions in the troposphere. Recent mass spectrometry measurements of tropospheric ions and recent laboratory investigations of their reaction rates make it possible to calculate the vertical profiles of positive and negative ion composition in the troposphere. The distribution of neutral parent constituents, a major requirement for ionic model study, has been calculated from a comprehensive two-dimensional model or is provided on the basis of observational data. Clustered aerosol ions have been proposed to be responsible for the heavy ions, which dominate near the surface. It has been predicted that, in most atmospheric environments, ions having ammonia and methyl cyanide as parent neutral species are not the major ions in the troposphere but that acetone and pyridinated clustered ions are the dominant ions. Pyridine cluster ions dominate below 6 km above which acetone cluster ions become the most abundant. However,

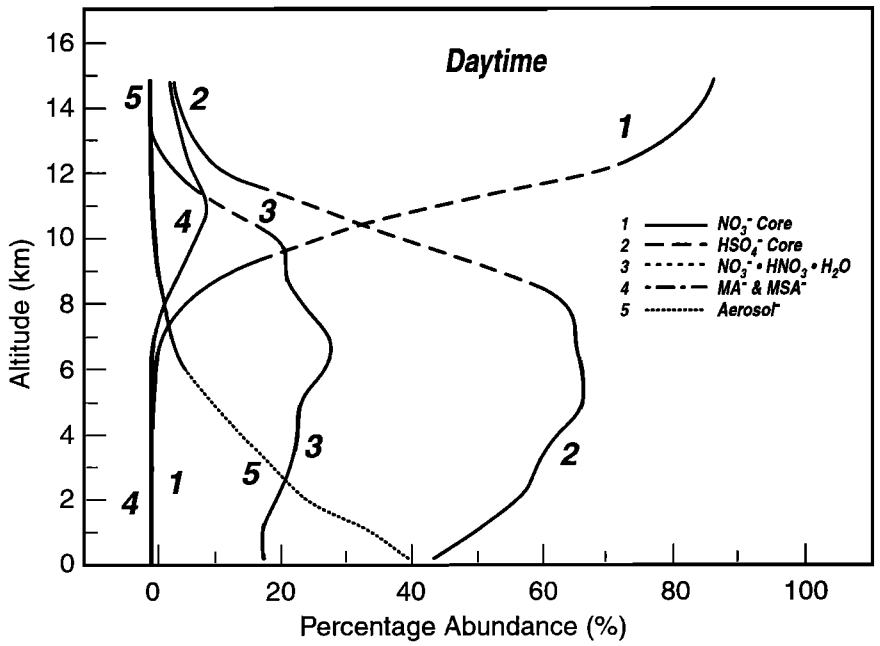

Figure 9. Height profiles of the percentage abundance of major negative ions calculated for observed daytime concentrations of H_2SO_4, MA, and MSA.

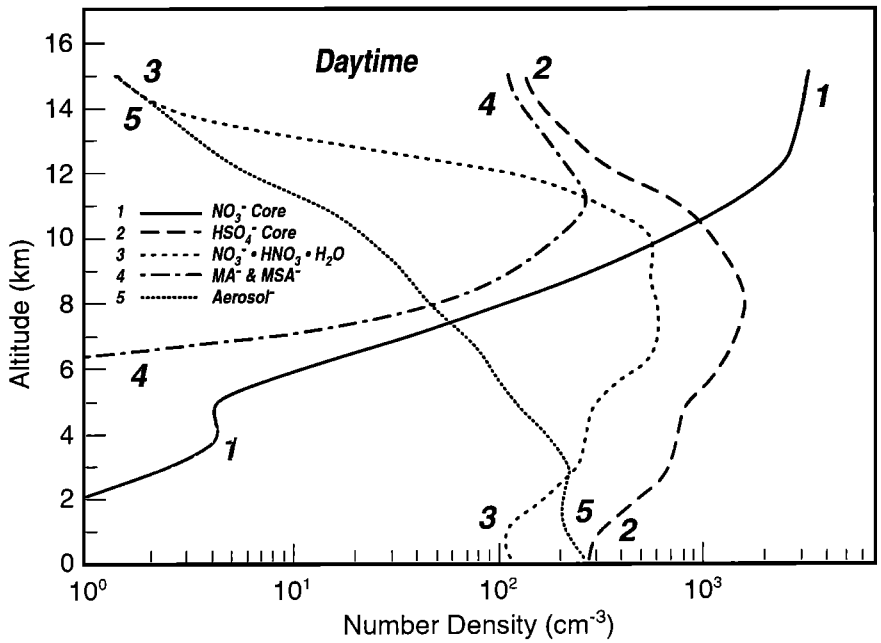

Figure 10. Vertical distribution of the concentration (cm^{-3}) of the major negative ions calculated for observed daytime values of H_2SO_4, MA, and MSA concentrations.

it should be emphasized that the concentration of pyridinated compounds is highly variable from one location to another and hence the concentration of pyridinated compounds could be low in remote (very clean) environments.

The model also shows that, for nighttime conditions, the dominant negative ions in the troposphere are of the type NO_3^- .HNO_3 H_2O and NO_3^- $(HNO_3)_n$. These results reproduce most of the observational data reported so far During daytime, when the concentration of parent neutrals (i e , H_2SO_4, MA, and MSA) appears to be much higher, the most abundant negative ions are provided by the HSO_4^--core ion family.

Finally, it is stressed that more observational data are required to evaluate these model results. Major emphasis should be given to the detection of the unidentified mass peaks in ion spectra and to the measurement of the alkaline compounds (especially pyridine, picoline and lutidine) in different atmospheric environments. The atmospheric abundance of these alkaline compounds is likely to increase with time as these are produced as a result of anthropogenic activities. As the concentration of parent neutral compounds varies considerably with space and is probably very different in industrialized and remote regions of the world, the spatial distribution of ions in the troposphere is expected to be nonuniform with local abundances that can be substantially different from those reported in this theoretical study. The model presented here should therefore be considered as a first attempt to represent the vertical distribution of positive and negative ions in the troposphere.

Acknowledgments. The authors are grateful to F. Eisele and G. Tyndall for their valuable comments and suggestions on early versions of the manuscript. G Beig is grateful to CSIR, New Delhi, for the financial assistance (project 03(0783)96/EMR/II) and to G B. Pant (Director, IITM) for his encouragement during the course of this work We acknowledge A. A Ursekar for her help in the preparation of this manuscript. The National Center for Atmospheric Research is operated by the University Corporation for Atmospheric Research under sponsorship of the National Science Foundation

References

Arijs, E , Stratospheric ion chemistry· Present understanding and outstanding problems, *Planet. Space Sci., 40*, 255-270, 1992

Arijs, E , and G Brasseur, Acetonitrile in the stratosphere and implications for positive ion composition, *J Geophys Res , 91*, 4003-4016, 1986

Arnold, F , Ion nucleation – A potential source for stratospheric aerosols, *Nature, 299*, 134-137, 1982

Arnold, F , H Heitmann, and K Oberfrank, First composition measurements of positive ions in the upper troposphere, *Planet Space Sci., 32* , 1567-1576, 1984

Arnold, F., G Knop, and H. Ziereis, Acetone measurements in the upper troposphere and lower stratosphere - Implications for hydroxyl radical abundances, *Nature, 321*, 505-507, 1986

Beig, G., and G Brasseur, Anthropogenic perturbations of tropospheric ion composition, *Geophys Res. Lett., 26*, 1303–1306, 1999.

Beig, G , S Walters, and G Brasseur, A two-dimensional model of ion composition in the stratosphere, 1, Positive ions, *J Geophys Res., 98*, 12,767-12,773, 1993a

Beig, G , S Walters, and G Brasseur, A two-dimensional model of ion composition in the stratosphere, 2, Negative ions, *J. Geophys Res., 98*, 12,775-12,781, 1993b.

Brasseur G., M. H Hitchman, S. Walters, M. Dymek, E. Falise, and M. Pirre, An interactive chemical dynamical radiative two-dimensional model of the middle atmosphere, *J. Geophys. Res , 95*, 5639-5655, 1990.

Datta, J., C P. Revankar, S. C Chakravarty, and A. P. Mitra, Influence of aerosols on middle atmospheric conductivities, *Phys. Scr., 36*, 705-710, 1987.

Eisele, F L , Direct tropospheric ion sampling and mass identification, *Int J. Mass Spectrom. Ion Phys , 54*, 119-126, 1983.

Eisele, F. L., Identification of tropospheric ions, *J Geophys Res., 91*, 7897-7906, 1986

Eisele, F L., First tandem mass spectrometric measurement of tropospheric ions, *J. Geophys. Res , 93*, 716-724, 1988

Eisele, F. L , Natural and transmission line produced positive ions, *J Geophys. Res., 94*, 6309-6318, 1989a

Eisele, F L., Natural and anthropogenic negative ions in the troposphere, *J Geophys. Res , 94*, 2183-2196, 1989b

Eisele, F. L , and E W. McDaniel, Mass spectrometric study of

tropospheric ions in the northeastern and southwestern United States, *J. Geophys. Res*, *91*, 5183-5188, 1986

Eisele, F. L., and D. J. Tanner, Identification of ions in continental air, *J. Geophys. Res.*, *95*, 20, 539-20, 550, 1990.

Eisele, F. L., and D. J. Tanner, Measurement of the gas phase concentration of H_2SO_4 and methane sulfonic acid and estimates of H_2SO_4 production and loss in the atmosphere, *J. Geophys Res.*, *98*, 9001-9010, 1993

Ferguson, E E, F. C. Fehsenfeld, and D. L. Albritton, Ion chemistry in the Earth's atmosphere, in *Gas Phase Ion Chemistry,* edited by M. T. Bowers, pp. 45-82, Academic, San Diego, Calif., 1979

Graedel, T. E., *Chemical Compounds in the Atmosphere,* pp., 440, Academic, San Diego, Calif, 1978

Hamm, S., and P. Warneck, The interhemispheric distribution and the budget of acetonitrile in the troposphere, *J. Geophys. Res., 95,* 20,593–20,606, 1990.

Hauck, G., and F. Arnold, Improved positive ion composition measurements in the upper troposphere and lower stratosphere and the detection of acetone, *Nature, 311*, 547-550, 1984

Hauglustaine, D A, G. P Brasseur, S Walters, P. J. Rasch, J.-F Müller, L K. Emmons, and M A. Carroll, MOZART, a global chemical transport model for ozone and related chemical tracers, 2, Model results and evaluation, *J. Geophys. Res, 103,* 28,291–28,335, 1998.

Heitmann, H, and F Arnold, Composition measurements of tropospheric ions, *Nature*, *306*, 747-751, 1983

Huertas, M. L., and J. Fontan, Evolution times of tropospheric positive ions, *Atmos Environ*, *9*, 1018-1026, 1975

Huertas, M. L., J. Fontan, and J Gonzalez, Evolution times of tropospheric negative ions, *Atmos. Environ*, *12*, 2351-2361, 1978,

Ingels, J., D Nevejans, P Frederick, and E Arijs, Acetonitrile and sulfuric acid concentrations derived from ion composition measurements during the MAP/GLOBUS 1983 Campaign, *Planet. Space Sci*, *35*, 685-691, 1987.

Jefferson, A., D J. Tanner, F. L. Eisele, D. D. Davis, G Chen, J. Crawford, J. W Huey, A L. Torres, and H. Berresheim, OH photochemistry and methane sulfonic acid formation in the coastal Antarctic boundary layer, *J Geophys. Res., 103*, 1647–1656, 1998.

Kawamoto, H, and T. Ogawa, First model of negative ion composition in the troposphere, *Planet Space Sci., 34*, 1229-1239, 1986

Knop, G., and F Arnold, Stratospheric trace gas detection using a new balloon-borne ACIMS-method: Acetonitrile, acetone, and nitric acid, *Geophys Res. Lett*, *14*, 1262-1265, 1987.

Lau, Y. K., S. Ikuta, and P Kebarle, Thermodynamics and kinetics of the gas phase reactions: $H_3O^+(H_2O)_{n-1} + H_2O = H_3O^+(H_2O))_n$, *J. Atmos. Chem. Soc., 104*, 1462-1469, 1982.

Luts, A., Evolution of negative small ions at enhanced ionization, *J Geophys. Res*, *100*, 1487-1496, 1995.

Luts, A., Temperature variation of the evolution of positive samll air ions at constant relative humidity, *J. Atmos Terr. Phys., 60*, 1739-1750, 1998.

Luts, A., and J. Salm, Chemical composition of small atmospheric ions near the ground, *J. Geophys. Res., 99*, 10,781-10,785, 1994.

Mauldin, R. L., III, D J. Tanner, J. A. Heath, B. J. Huebert, and F. L. Eisele, Observations of H_2SO_4 and MSA during PEM-Tropics A, *J. Geophys Res., 104*, 5801–5816, 1999

Mohnen, V. A, Discussion of the formation of major positive and negative ions up to the 50 km level, *J. Appl. Geophys*, *84*, 141-153, 1971.

Perkins, M D., and F L. Eisele, First mass spectrometric measurements of atmospheric ions at ground level, *J. Geophys. Res., 89*, 9649-9657, 1984.

Rosen, J M., and D. J. Hofmann, A search for large ions in the stratosphere, *J. Geophys. Res., 93*, 8415-8422, 1988.

Rosen, J. M., D J Hofmann, and W. Gringel, Measurements of ion mobility to 30 km, *J. Geophys. Res., 90*, 5876-5884, 1985

Schlager, H., R Fabian, and F Arnold, A new cluster ion source / ion drift cell apparatus for atmospheric ion studies - First mobility and reaction rate coefficient measurements, in Proc. of the 3rd Int. Swarm Seminar, Innsbruck, Austria, pp 257-262, 1983.

Schneider, J, V Bürger, and F. Arnold, Methyl cyanide and hydrogen cyanide measurements in the lower stratosphere: Implication for methyl cyanide sources and sinks, *J. Geophys. Res., 102*, 25,501–25,506, 1997

Singh, H B., D. O'Hara, D Herlth, W. Sachse, D. R. Blake, J D. Bradshaw, M Kanakidou, and P. J. Crutzen, Acetone in the atmosphere. Distribution, sources, and sinks, *J. Geophys. Res*, *99*, 1805–1819, 1994.

Snider, J. R, and G. A. Dawson, Surface acetonitrile near Tucson, Arizona, *Geophys. Res. Lett., 11*, 241–242, 1984.

Tanner, D J, and F L. Eisele, Ions in oceanic and continental air mass, *J. Geophys. Res*, *96*, 1023-1031, 1991.

Turco, R. P, J.-X. Zhao, and F. Yu, A new source of tropospheric aerosols: Ion–ion recombination, *Geophys Res. Lett., 25*, 635-638, 1998.

Viggiano, A A, R. A Perry, D. L. Albritton, E. C. Ferguson, and F C. Fehsenfeld, Stratospheric negative-ion reaction rates with H_2SO_4, *J Geophys Res*, *87*, 7340- 7342, 1982

Viggiano, A. A., R A. Morris, F. Dale, and J. F. Paulson, Tropospheric reactions of $H^+(NH_3)_m(H_2O)$ with pyridine and picoline, *J Geophys Res*, *93*, 9534-9538, 1988a.

Viggiano, A. A., F Dale, and J F. Paulson, Proton transfer reactions of $(H_2O)_{n=2-11}$ with methanol, ammonia, pyridine, acetonitrile and acetone, *J. Chem. Phys.*, *88*, 2469-2477, 1988b.

Ziereis, H, and F. Arnold, Gaseous ammonia and ammonium ions in the free troposphere, *Nature*, *321*, 503-505, 1986.

Yu, F, and R P Turco, Ultrafine aerosol formation via ion-mediated nucleation, *Geophys Res Lett.*, 27, 883-886, 2000

G. Beig, Indian Institute of Tropical Meteorology, Pune-411 008, India. (email: beig@tropmet ernet.in)

G. Brasseur, Max Planck Institute for Meteorology, D-20146 Hamburg, Germany (email: brasseur@dkrz.de)

(Received September 15, 1999; revised February 4, 2000; accepted February 14, 2000)